WORKING PAPERS

N° 1410

February 2023

# “Discrete and Smooth Scalar-on-Density Compositional Regression for Assessing the Impact of Climate Change on Rice Yield in Vietnam”

Thi-Huong Trinh, Christine Thomas-Agnan and Michel Simioni

Toulouse School of Economics

# Discrete and smooth scalar-on-density compositional regression for assessing the impact of climate change on rice yield in Vietnam

Huong Trinh Thi[1*†], Christine Thomas-Agnan[2] and Michel Simioni[2,3††]

[1*]Faculty of Mathematical Economics, Thuongmai University, Ho Tung Mau street, Hanoi, 10000, Vietnam.
[2]Toulouse School of Economics, University of Toulouse Capitole, Toulouse, 31000, France.
[3]MoISA, University of Montpellier, Place Pierre Viala, Montpellier, 34060, France.

*Corresponding author(s). E-mail(s): trinhthihuong@tmu.edu.vn;
Contributing authors: christine.thomas@tse-fr.eu;
michel.simioni@inrae.fr ;
†These authors contributed equally to this work.

**Abstract**

Within the econometrics literature, assessing the impact of climate change on agricultural yield has been approached with a linear functional regression model, wherein crop yield, a scalar response, is regressed against the temperature distribution, a functional parameter alongside with other covariates. However this treatment overlooks the specificity of the temperature density curve. In the realm of compositional data analysis, it is argued that such covariates should undergo appropriate log-ratio transformations before inclusion in the model. We compare a discrete version with temperature histograms treated as compositional vectors and a smooth scalar-on-density regression with temperature density treated as an object of the so-called Bayes space. In the latter approach, when density covariate data is initially available as histograms, a preprocessing smoothing step is performed involving CB-splines smoothing. We investigate the respective advantage of the smooth and discrete approaches by modelling the impact of maximum and minimum daily temperatures on rice yield in Vietnam. Moreover we advocate for the modelling of climate change scenarios through the introduction of perturbations of the initial density, determined by a change direction curve computed from the IPPC scenarios. The resulting impact on rice yield is then quantified by calculating a simple inner product between the parameter of the density covariate and the change direction curve. Our findings reveal that the smooth approach and the discrete counterpart yield coherent results, but the smooth seems to outperform the discrete one by an enhanced ability to accurately gauge the phenomenon scale.

**Keywords:** Compositional scalar-on-density regression, Bayes space, compositional splines, functional regression, climate change, rice yield, Vietnam.

# 1 Introduction

We consider improving the linear functional regression models approach used in the econometrics literature to assess the impact of climate change on agricultural yield by properly taking into account the density nature of their functional parameter.

As the complexity of recorded data continues to grow, contemporary models increasingly involve intricate data objects including random densities. We are focusing here on regression models where such density objects serve as explanatory variables. These density objects can be treated either in a discrete fashion as histograms or in a continuous fashion as density functions, see for example [1]. True continuous observations are rarity. Density data, often available in the discrete form of histograms, are typically treated as continuous when the number of bins is exceedingly large. Consequently, a preprocessing step involving smoothing becomes necessary.

It is often the case that density data are recorded in an aggregated form as histograms, see for example [2] for a comprehensive review in the context of climate change econometrics. When adopting this discrete approach, the sample space can be described by the set of vectors of bin frequencies (percentages), with positive components that sum to one. These vectors are called compositions and their space is known as a simplex. A proper statistical treatment of this type of data can be done by compositional data analysis, see [3] or [4] for an introduction. Scalar-on-composition regression models using the simplex representation are described for example in [5]. They are obtained by transforming the simplex explanatory vectors, usually using a log-ratio transformation, to map them into an unconstrained linear space $\mathbb{R}^k$ (for some adapted value of $k$).

Conversely, [6] conducts a comprehensive review of various methodologies for constructing regression models involving samples of probability density functions with a functional perspective. In the realm of functional data analysis, densities stand out as unique entities due to the constraints they must satisfy. For one-dimensional densities, the sample space can be defined as the space $\mathcal{D}$ of functions with positive values and a unit integral. [6] highlights one of the two primary approaches, which revolves around the representation of densities in the so-called Bayes spaces $\mathcal{B}^2$. Bayes spaces, initially introduced by [7], then extended in [8], endow the space $\mathcal{D}$ of densities with a finite support $[a, b]$ with a Hilbert space structure. This space and structure can be viewed as a continuous version of the simplex and its associated operations. As for the log-ratio transformation, the functional centered log-ratio serves as the functional counterpart of the classical centered log-ratio transformation for vectors of a simplex. This concept is used for example in [9] to construct functional scalar-on-density regression models. For the preprocessing step, [10] propose a new class of splines, known as compositional splines or CB-splines, specifically designed to accomodate the density constraints.

Nonetheless the functional (smooth) approach implementation is more complex prompting the natural question of assessing the potential advantage gained from using the functional model. Our first objective in this work is to explore this comparison through an original application to the study of the impact of climate change on rice yield in Vietnam. Our second goal is to provide tools to assess the marginal impact of climate change on rice yield.

Using regression models to relate agricultural yield and climate descriptors is by no means a new endeavor, as evidenced by [11]. Climate change exerts both direct and indirect impacts on various facets of the food system encompassing food production, storage, processing, distribution, retail and consumption, as discussed by [12]. Due to its direct exposition to weather conditions, crop production is all the more sensitive to climate change. In countries such as Vietnam, crop production plays a vital role in both the country's economy and the well-being of its people. For instance, rice cultivation occupies a substantial 63% of Vietnam's total agricultural land and is also essential to the livelihoods of 63% of Vietnamese farming households. Moreover, in 2019, rice production in Vietnam reached a staggering 43.4 million tons, solidifying the country's position as the world's fifth-largest rice producer and second-largest rice exporter. Unfortunately, this critical sector faces mounting threats from climate change. The rising sea levels pose a significant danger to Vietnam's primary rice-growing region, the Mekong River Delta, which accounts for 54.47% of the nation's rice-planted area. Under a high greenhouse gases global emissions scenario, sea levels could rise by up to 84 cm, potentially submerging large portions of the Delta plain whose estimated average elevation is expected to fall around 80cm below sea-level by the end of the century [see Chapters 1 and 3 in 13]. Furthermore, temperature projections (ranging from a modest increase of approximately 1.3°C under a low greenhouse gases global emissions scenario to substantial rise of around 4.2°C under a high emissions scenario, with faster increases on the North of the country than in the South) signal the possibility of chronic heat stress in some areas that could also adversely affect rice production, even under lower emissions pathways.

Within the field of econometrics, assessing the impact of climate change for a given economic sector relies on the specification and estimation of a damage function. For a specific outcome, the damage function relates a change in the climate indicators to the corresponding change in the outcome. [14] present empirical, micro-founded sector-specific damage functions tailored to various sectors, including agriculture, crime, health and labor. Several of these damage functions consider crop yield as the outcome of interest and link that yield to temperature and precipitation. Noteworthy among these contributions are the insights provided by [15], while a recent and comprehensive survey can be found in [16]. [15] build their assumptions on the premise that temperature effects on yields accumulate over time and that yield is proportional to total exposure. The consequence of this assumption is that we may use the temperature density as a functional covariate instead of using the times series of temperatures, in other words the order in time in which the temperatures occur has no impact on the yield. In mathematical terms, this assumption allows to specify the link between crop yield (a scalar response) and temperature as a linear functional of a probability density function. This functional incorporates an integral of the temperature density against a regression parameter, itself a function of temperature. This regression parameter encapsulates the sensibility of crop yield at different temperature levels. Similar models are considered for example in [17] where the functional covariate is also temperature but regarded as a function of time whereas we use the temperature density curve. The estimation strategy adopted by [15] revolves around using a discrete approximation of the rigth hand side integral resulting from approximating the temperature density by an histogram of the number of days falling into different temperature bins over the crop growing season. Similar to the handling of dummy variables, one bin is omitted from the list of regressors to account for the fact that the sum of the regressors remains constant and equal to the total number of days in the crop growing season. The impact of an additional day within a specific temperature bin is therefore measured in reference to the omitted bin. This estimation strategy has been adopted by several researchers, gaining prominence after its use in [18]. For instance, [19] applied this approach in their study of how subsistence Peruvian farmers respond to extreme heat.

The estimation strategy proposed by [15] can be discussed in light of recent contributions to the statistical literature. The original model of [15] uses a function representation for the temperature density, making the model directly comparable to the functional scalar-on-density approach. In both cases the density function appears on the right hand side of the regression equation in a linear fashion through an integral term. In Schlenker and Robert's treatment of their model, they approximate this integral by a finite sum resulting in a regression model on bin frequencies (excluding a reference bin). This implementation of their model is therefore comparable to a discrete scalar-on-composition model. However a significant divergence arises from this point onward. Schlenker and Robert's model uses bin frequencies (except the reference bin) as explanatory variables in a linear model. It has long been recognized in the statistical literature, see for example [20], that comparing densities is best achieved by using relative distributions i.e. the ratio of their densities. Consequently when comparing temperature distributions, it is advisable to employ relative densities instead of absolute differences between them. While using linear effects of the temperature bin frequencies as in [15] is coherent with absolute differences, in contrast, compositional data analysis use log-ratios of bin frequencies as explanatory variables, aligning with the notion of relative differences.

The paper is organized as follows. Section 2 reviews the methodological tools involved in these discrete and smooth compositional models (simplex space and Bayes space structures, centered log-ratio transformations) as well as the construction of the compositional splines. Section 3 presents the rice yield data and the weather data and explores their main features. Section 4 presents the discrete and smooth compositional scalar-on-density regression models and their estimation results. It also provides an interpretation of the discrete and smooth parameters associated to the temperature distribution parameters. Section 5 presents our proposal to derive the formulas for computing the impact of a climate change scenario and its variance. Based on the model fit, we perform the computations for the RCP2.6 scenario provided by IPPC for the end of the century. An illustration of these impacts on the dataset allows to reveal the interest of the smooth approach. Section 6 then concludes.

# 2 Methodological reminders

The dataset central to our problem comprises distributions of maximum and minimum daily temperatures spanning a 30-year period, from 1987 to 2016, across 63 provinces in Vietnam. These temperature density distributions serve as key covariates within our regression model, designed to uncover the factors influencing rice yield in Vietnam over this timeframe. In the discrete approach, we represent these temperature covariates as compositional vectors and and we provide an overview of fundamental techniques for working with compositional vectors in Section 2.1. In the smooth approach, we use smooth densities and we remind in Section 2.2 the construction of the Bayes space $\mathcal{B}^2$ of densities. As we delve into the regression component, for the discrete approach, we employ scalar-on-composition regression techniques, as presented by [5]. In contrast, since the density covariate data is originally available as an histogram, the regression part of the functional approach necessitates a preliminary step to transform the histograms into $\mathcal{B}^2$ elements using CB-splines smoothing. We briefly review CB-splines in Section 2.3 and CB-splines smoothing in Section 2.4.

## 2.1 Discrete densities as compositional vectors

Let us first recall that compositional data (hereafter referred to as CoDa) vectors can be defined as vectors consisting of $D$ positive components that sum up to one, elements of a simplex denoted by $\mathcal{S}^D$. A discrete density function associated to a random variable with a finite number of outcomes is typically represented by its probability mass function, or equivalently by the vector of probabilities of each of these outcomes which satisfies the same constraints as a CoDa vector. This space can be equipped with a vector space structure using the following operations, see e.g. [3].

1. $\oplus$ is the perturbation operation, corresponding to the addition in $\mathbb{R}^D$:

$$\text{For} \quad \mathbf{u}, \mathbf{v} \in \mathcal{S}^D, \mathbf{u} \oplus \mathbf{v} = \mathcal{C}(u_1 v_1, \ldots, u_D v_D),$$

2. $\odot$ is the power operation, corresponding to the scalar multiplication in $\mathbb{R}^D$:

$$\text{For} \quad \lambda \in \mathbb{R}, \mathbf{u} \in \mathcal{S}^D \quad \lambda \odot \mathbf{u} = \mathcal{C}(u_1^\lambda, \ldots, u_D^\lambda),$$

where $\mathcal{C}$ denotes the closure of a vector (division by the sum of its components).
The above operations enable the definition of a meaningful average of a sample of $n$ compositional vectors $\mathbf{u}_i$ (for $i = 1$ to $n$) by $\bar{\mathbf{u}} = \frac{1}{n} \odot (\mathbf{u}_1 \oplus \ldots \oplus \mathbf{u}_n)$ (thus the components of this average are the geometric averages of the corresponding sample's components).

The clr transformation of a vector $\mathbf{u} \in \mathcal{S}^D$ is defined by

$$\mathrm{clr}(\mathbf{u}) = \mathbf{G}_D \ln \mathbf{u},$$

where $\mathbf{G}_D = \mathbf{I}_D - \frac{1}{D}\mathbf{1}_D{\mathbf{1}_D}^T$, $\mathbf{I}_D$ is a $D \times D$ identity matrix, $\mathbf{1}_D$ is the $D$-vector of ones and where the logarithm of $\mathbf{u} \in \mathbf{S}^D$ is understood componentwise. For a vector $\mathbf{u}^*$ in the orthogonal space $\mathbf{1}_D^\perp$ (orthogonality with respect to the standard inner product of $\mathbb{R}^D$), the inverse clr transformation is defined by

$$\mathrm{clr}^{-1}(\mathbf{u}^*) = \mathcal{C}(\exp(\mathbf{u}^*)).$$

The simplex $\mathcal{S}^D$ of dimension $D-1$ can be equipped with the Aitchison inner product

$$< \mathbf{u}, \mathbf{v} >_A = < \mathrm{clr}(\mathbf{u}), \mathrm{clr}(\mathbf{v}) >,$$

where the right hand side inner product is the standard inner product in $\mathbb{R}^D$.

### 2.2 Continuous densities as elements of the Bayes space

As outlined in [10], density functions supported in a bounded interval $[a,b]$ can be regarded as elements of the so-called Bayes space denoted by $\mathcal{B}^2([a,b])$ and comprising positive functions integrating to one on $[a,b]$ whose log-transform is square integrable. This concept corresponds to a particular case of that introduced in [8] for the reference measure being the Lebesgue measure.

This space can first be equipped with a vector space structure using the following operations. For any positive function $f$ on $[a,b]$, the closure $\mathcal{C}(f)$ of $f$ is the unique density proportional to it. Subsequently, for any two functions $f$ and $g$ in $\mathcal{B}^2([a,b])$ and any real $\alpha$, the following operations can be defined

- perturbation as $(f \oplus g)(t) = \mathcal{C}(f(t)g(t))$
- powering as $(\alpha \odot f)(t) = \mathcal{C}(f(t)^\alpha)$

The centered log-ratio (clr) transformation is defined for $f \in \mathcal{B}^2([a,b])$ and $t$ in $[a,b]$ by

$$\mathrm{clr}f(t) = \log f(t) - \frac{1}{b-a}\int_a^b \log f(u)du \qquad (1)$$

Through its construction, the clr transformation maps $\mathcal{B}^2([a,b])$ into the space $L_0^2([a,b])$ of square integrable functions on $[a,b]$ with a zero integral. The inverse transformation is well defined and can be expressed as follows for a function $f_0 \in L_0^2([a,b])$,

$$\mathrm{clr}^{-1}(f_0)(t) = \mathcal{C}\exp\left(f_0(t)\right).$$

$\mathcal{B}^2([a,b])$ can then be equipped with an inner product rendering the clr transformation isometric, for a corresponding choice of inner product in $L_0^2([a,b])$. We adopt the definition in [10] for the $\mathcal{B}^2([a,b])$ inner product, which differs by a constant from the inner product introduced in [8]:

$$< f, g >_{\mathcal{B}^2} = \int_a^b \mathrm{clr}f(t)\ \mathrm{clr}g(t)dt = < \mathrm{clr}f, \mathrm{clr}g >_{L_0^2([a,b])}. \qquad (2)$$

### 2.3 Reminder on CB-splines and ZB-splines

Spline functions are constructed by piecing together segments of polynomials of a specified degree connecting at specified knots points while adhering to prescribed smoothness conditions [see e.g. 21]. In our context, aimed at approximating density functions, we require a specific type of constrained splines. One approach to constructing them is described in [10] using the so-called ZB-splines in $L_0^2([a,b])$ and corresponding CB-splines in $\mathcal{B}^2([a,b])$. As is common in many CoDa techniques, the procedure is based on a log-ratio transformation, specifically the clr introduced in Section 2.2. The process starts by constructing a basis of spline functions that fulfill the integral constraint within $L_0^2([a,b])$. These basis functions are then pulled back to $\mathcal{B}^2([a,b])$ by the inverse clr transformation.

For a given order $d$ and a knot sequence $\Lambda = \{(\lambda_1, \ldots, \lambda_g) : a < \lambda_1 < \ldots \lambda_g < b\}$ whose elements are called inside-knots, let $S_d^\Lambda$ be the subspace of $L^2([a,b])$ of polynomial splines or order $d$ (degree $k = d-1$) and inside-knots $(\lambda_1, \ldots, \lambda_g)$, see [22] for a complete description. $S_d^\Lambda$ has dimension $d+g$ and its most popular basis is given by the set of so-called (normalized) B-splines functions which have a small support and good computational properties. For technical reasons, additional knots are introduced at the boundary: if $k$ is the degree of the polynomial pieces ($d = k+1$ the corresponding order), $k$ knots equal to $a$ are added at the beginning of the interval and $k$ knots equal to $b$ at the end. [10] construct a basis of so-called ZB-splines for the subspace $\mathcal{Z}_d^\Lambda = S_d^\Lambda \cap L_0^2([a,b])$ of dimension $g+k$, the loss of one dimension being due to the zero-integral constraint. The inverse clr of the ZB-basis functions are called the CB-basis functions. For this application, we use exclusively cubic splines for which $k = 3$ and $d = 4$. Equation (17) in [10] establish a correspondence between the representation of any function in $\mathcal{Z}_d^\Lambda$ within both basis systems. This correspondence proves invaluable as it facilitates the manipulation of ZB-splines using conventional code originally designed for B-splines.

In our subsequent application, the temperature data will first be processed into a set of histograms, each depicting daily maximum and minimum temperatures for a specific province and year. For maximum temperatures, the data is discretized into 28 bins of length 1 within the interval $[a,b] = [12,40]$. To approximate the underlying densities represented by these original histograms, we employ cubic splines ($k = 3$) and set $g = 7$ (respectively $g = 9$) as the number of inside knots for illustrative purposes. Consequently, the dimension of the ZB-spline basis becomes $7 + 3 = 10$ when using 7 inside knots (respectively $9 + 3 = 12$ for 9 inside knots). For minimum temperatures, the data is discretized into 22 bins of length 1 within the interval $[a,b] = [7,29]$.

In both cases, the positioning of the knots is determined relative to the data points position using quantiles as argued in [10].

Figure 1 represents the two sets of basis functions (for maximum temperature) thus obtained in $L_0^2([a,b])$ and in $\mathcal{B}^2([a,b])$. The vertical dotted lines on the plots indicate the knots position. We observe that the inclusion of two additional knots in the lower plots results in an increased number of basis functions that concentrate around the mode of the distribution. This enhancement enables a more precise approximation of the densities, particularly in regions where our dataset features a higher density of temperature data points.

**Fig. 1** CB-splines (left) and ZB-splines (right) with 7 inside knots (top) and 9 inside knots (bottom)

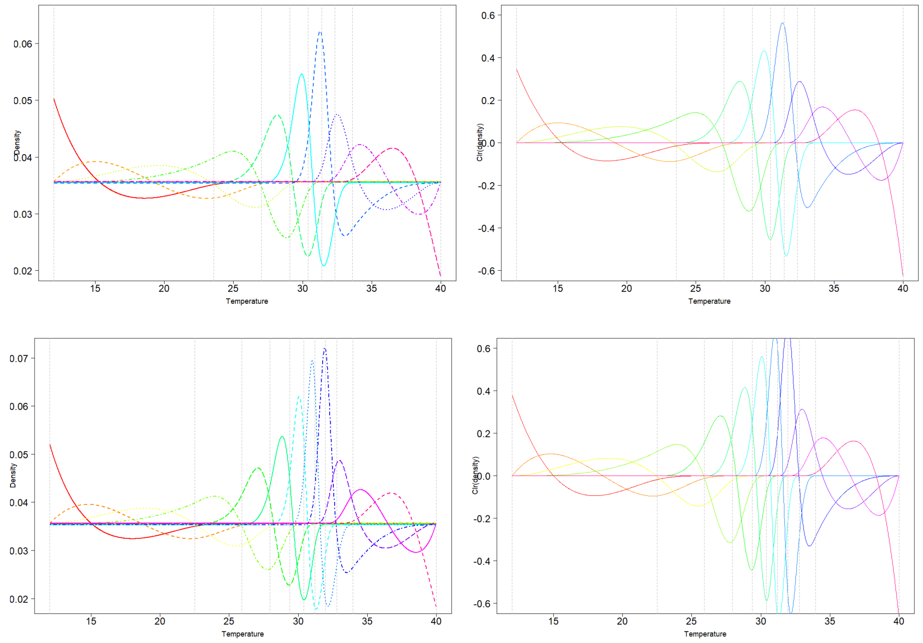

## 2.4 Smoothing histograms with CB-splines

Our original temperature data comprises sequences of daily maximum and minimum temperatures. In order to apply the same technique as [10], we first preprocess the data into intermediate histogram representations subsequently transformed into smooth density functions using CB-splines as in [23]. The CB-spline smoothing step involves choosing a ZB-spline basis in $L_0^2$ and viewing the estimation of the clr transformed densities expressed in the ZB-basis as a penalized least squares regression. This regression smooths the scatterplot of the clr transformed histogram frequencies as a function of the ZB-spline basis functions evaluated at the midpoints of the histograms bins. To ensure the existence and uniqueness of the least squares problem (full column rank of the collocation matrix), we enforce an upper limit on the number of knots. This upper bound is dictated by the Schoenberg-Whitney conditions (see [24]). In our application, the condition, both for maximum and minimum temperature, stipulates in particular that the number of knots must be less than or equal to the number of bins minus 3 (degree of splines). Smoothing with ZB splines does not accommodate bins with zero counts because of the log transformation. To address this limitation, we implement a simple zero-replacement procedure: any zero count is substituted by $10^{-7}$ after which we apply the closure operator. For the selection of the smoothing parameter, we opt for a generalized cross-validation using a regular grid of 100 points on a log-scale.

As an illustrative example, Figure 2 displays the histogram of the daily maximum temperatures in 1995 in the Yen Bai province (North-East of Vietnam), as well as the corresponding smooth density obtained by the above procedure on the left plot, and the smoothed clr transform on the right plot.

**Fig. 2** Density of daily maximum temperature in 1995 in Yen Bai province (left) and its clr transform (right)

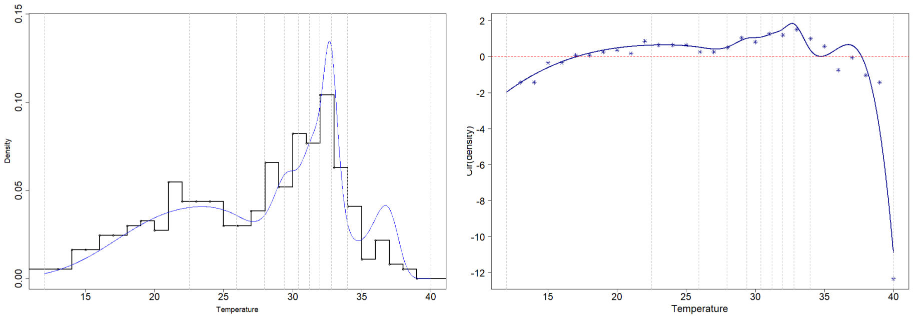

# 3 Data and exploratory analysis

## 3.1 Rice yield data

The dataset concerning rice yield is sourced from the International Rice Research Institute[1]. The data set contains comprehensive information on annual rice production, harvested area, and rice yield at provincial level from 1987 to 2016. Rice yield is quantified in tons per hectares. Figure 3 provides an overview of the overall evolution of rice yield over the considered period. After a period of stagnation between 1987 and 1992, rice yield has exhibited consistent growth since 1992, affecting all Vietnamese provinces. This growth may be attributed to the progress of agronomic techniques over the years. While we lack a direct proxy for this progress, we will account for it through the incorporation of a linear time trend. This choice is supported by Figure 4, which reports the evolution of average rice yields for the six different agronomic regions in Vietnam. In this figure, we use the following acronyms for the regions: NMM for Northern Midland and Mountainous region, NCC for North Central Coast region, CHR for Central Highlands region, SR for Southeast region, MDR for Mekong Delta River region and RRD for Red River Delta region.

## 3.2 Weather data

The weather data used in this study encompasses daily maximum and daily minimum temperatures and precipitation records. Temperature data comes from the Climate Prediction Center (CPC) database developed and maintained by the National Oceanic and Atmospheric Administration (NOAA). We have retrieved historical information pertaining to daily maximum temperatures for a grid with a resolution of $0.50 \times 0.50$

[1] IRRI is an organisation that promotes research and development of rice production in the world. Information about the institute can be found at https://www.irri.org/

**Fig. 3** Rice yield distributions from 1987 to 2016

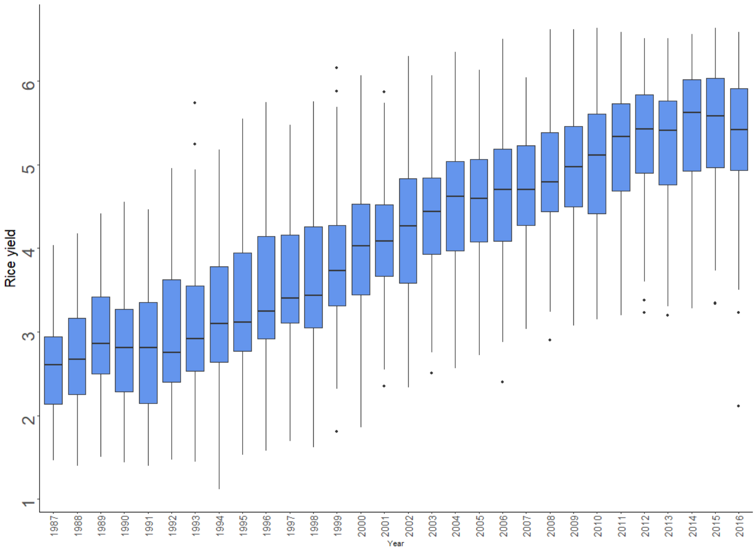

**Fig. 4** Average rice yield by agronomic regions from 1987 to 2016

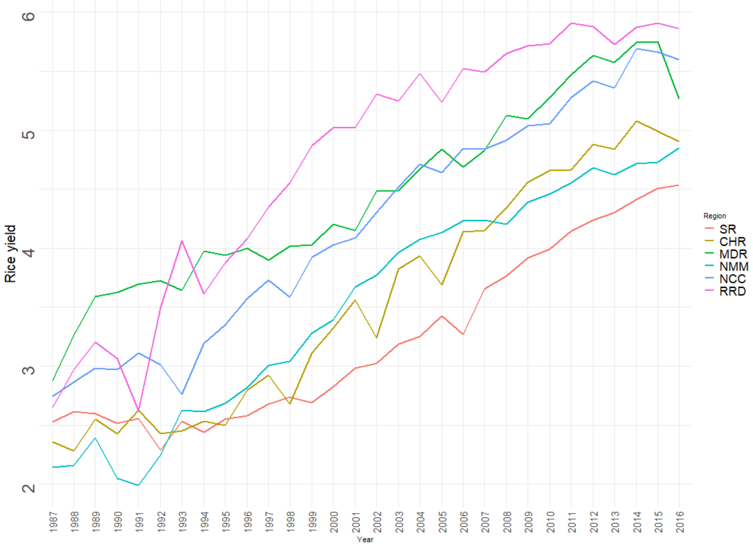

degrees of latitude and longitude, specifically for the geographical expanse of Vietnam. Subsequently, we have transformed this data to yield the daily maximum temperature for each of 63 Vietnamese provinces and during a period of 30 years (1987-2016) (365 or 366 values for each year). The compilation yields one temperature distribution for each of 1890 statistical units.

Figure 5 displays the average histograms of each of the 6 regions where average is understood with the simplex operations as defined in Section 2.1. These histograms

**Fig. 5** Maximum temperature histograms across the Vietnamese regions in 2015

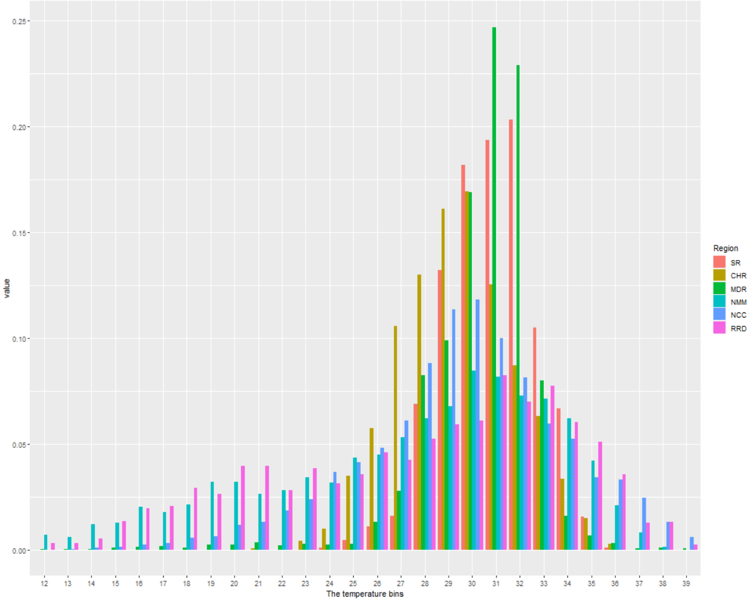

provide a visual representation of how the range of maximum temperatures varies across different regions, emphasizing the substantial regional disparities.

Using the CB-spline smoothing tool we can also explore other aspects of the temperature densities variations across time and space. Figure 6 displays the daily maximum temperature density with 9 knots (along with its clr transform) in the province of Ninh Binh which is one of the major provinces for rice production situated in the RRD region. We use the viridis color palette with 30 values, featuring 30 distinct values that transition from yellow in 1987 to dark violet in 2016 with intermediate shades of green. The top part of Figure 6 clearly reveals the rightward shift of the temperature densities corresponding to climate change. Finally Figure 7 displays the densities and their clr transforms for all provinces in the year 2015 (9 inside knots). When examining the clr transforms, we can see groups of provinces and it would be interesting to explore their respective spatial position. It seems that they primarily differ in the range of the observed maximum temperatures.

To facilitate the integration of the smoothed histograms into the subsequent regression model, it is imperative to ensure that they are expressed in the same basis of CB-splines. Consequently, we must employ a consistent set of knots across all $63 * 30 = 1890$ histograms. For this reason, we first pool all observations into a single distribution and place the knots at the quantiles of this global distribution.

Improving this phase of the process hinges on obtaining information about the specific starting and ending dates of the growing season within each province. However since these temporal boundaries may exhibit substantial variability across geographical regions as we have seen in section 3.2, the adoption of a standardized temperature

**Fig. 6** Density (top panel) and clr transform (bottom panel) of the smoothed daily maximum temperature from 1987-2016 in Ninh Binh province

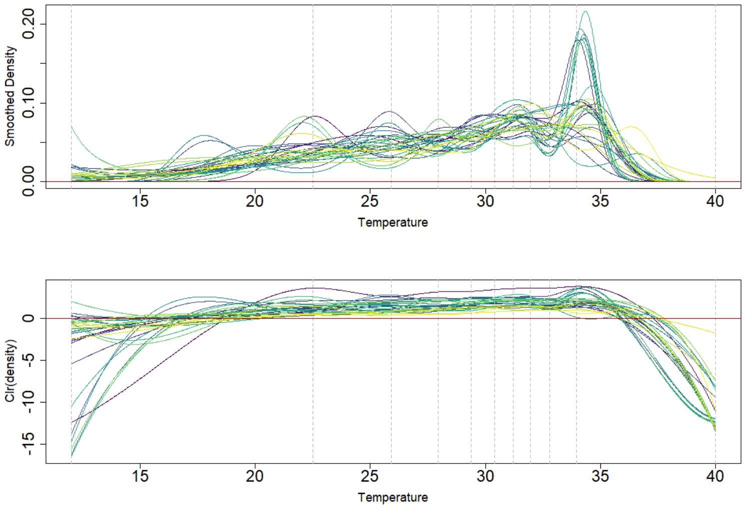

**Fig. 7** Density (top) and Clr transform (bottom) of the smoothed daily maximum temperature from in 2015 for all provinces

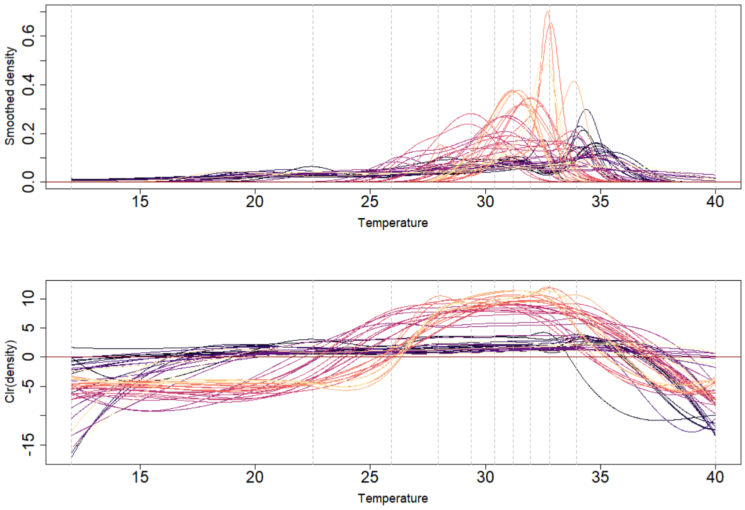

range across all provinces would then be rendered difficult, unless we find a way of overcoming this technical constraint.

## 3.3 Climate change data

Let us first examine the "historical" climate change between 1987 and 2016. Using relative distributions for comparing two distributions as recommended by [20], Figure 8 showcases boxplots depicting the ratios of 2016 to 1987 densities across provinces in some regions for maximum and minimum temperatures. Notably, this analysis highlights temperature ranges affected by changes, specifically ranging from 26 to 40 degrees Celsius for maximum temperature and 17 to 29 degrees Celsius for minimum temperature. Moreover for maximum temperature in the RRD and MDR regions, a concentration of temperature increase is observed within the 27 to 33 degrees Celsius range. In contrast, for minimum temperature, we observe an increasing trend of the ratio indicating a shift of this density to the right.

**Fig. 8** Relative distribution of daily temperature for 2016 versus 1987 in some regions

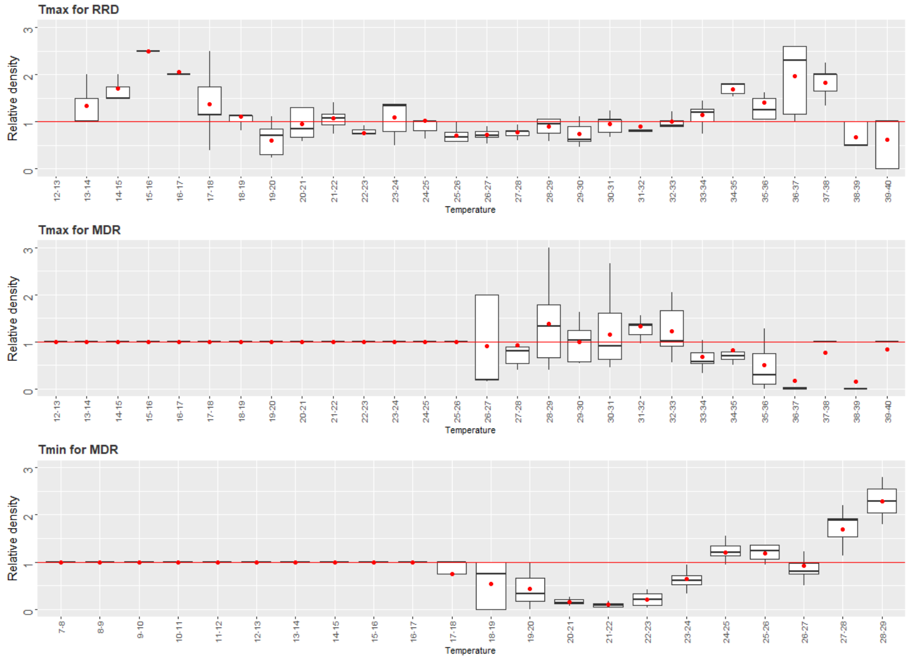

The Intergovernmental Panel on Climate Change (IPCC) provides projections of global $CO_2$ emissions and associated temperature distributions around the world under several scenarios associated to representative concentration pathways (RCPs) for the end of this century, see for example [25]. In Section 5,, we will use the most optimistic RCP called RCP2.6, which projects an average increase of 1 degree Celsius relative to the period 1986-2005. The RCP2.6 data for vietnamese provinces come from [26].

# 4 The discrete and smooth regression models

The objective in this application is to develop a regression model to unravel the relationship between rice yield and the distribution of daily maximum and minimum temperatures for the corresponding year and province, while also controlling for additional covariates. Unlike a conventional time series model used for yield prediction in the future, our focus here is to leverage spatio-temporal variability to quantify the influence of temperature on rice yield. Therefore we decide to include a simple linear time trend in the model as a proxy for unobserved factors that may have evolved over time, such as advancements in production techniques. In view of Figures 3 and 4, the inclusion of a linear trend appears to be a reasonable choice. We further use other controlling factors namely precipitation and regional dummies. Given the distributional nature of our primary covariate, we need an adapted regression model. The choice boils down to either utilizing a histogram of daily temperatures as a compositional covariate, akin to the approach in [5], or opting for a smoothed representation of the temperature density as a continuous density covariate, following the method outlined in [9]. Before delving into the results, let us first revisit the fundamental principles behind these two models.

## 4.1 The discrete regression model

The scalar-on-composition regression model as presented for example in [5] constitutes a regression framework where at least one of the covariates takes the form of a compositional vector. In our discrete regression setup, the compositional vectors are temperature histograms which can also be viewed as discrete densities. Any linear function of a compositional explanatory variable $\mathbf{X} \in \mathcal{S}^D$ must be of the form $< \beta, \mathbf{X} >_A$, where $\beta$ is a parameter vector of $\mathcal{S}^D$ and $< .,. >_A$ is the classical Aitchison inner product in $\mathcal{S}^D$ (see e.g. [4]). Therefore a linear model designed to explain a scalar variable $Y$ with possibly several compositional variables $\mathbf{X}_j \in \mathcal{S}^{L_j}$ for $j = 1, \dots J$ and several scalar variables $\mathbf{Z}_l$ for $l = 1, \dots L$ is formulated by an equation of the form

$$Y_i = \alpha + \sum_{j=1}^{J} < \boldsymbol{\beta}_j, \mathbf{X}_{ij} >_A + \sum_{l=1}^{L} \gamma_l \mathbf{Z}_{il} + \epsilon_i, \tag{3}$$

where the parameters $\beta_j \in \mathcal{S}^{L_j}$ and the errors $\epsilon_i$ are i.i.d. gaussian variables with mean zero and variance $\sigma^2$. For our application, it is essential to index all observations according to both the province $i$ and the year $k$ therefore the single index $i$ of equation (3) is from now on replaced by the two indices $i$ and $k$. This adjustment allows us to define $Y_{ik}$ as the rice yield for province $i$ (ranging from 1 to 63) in year $k$ (spanning from 1 to 30). Initially, the model comprises several classical scalar variables ($L = 7$) including time, precipitation and five regional dummies (reference region being CHR). In addition to these, we also incorporate two discrete densities as compositional covariates, namely the histograms of maximum and minimum daily temperature, reported with equal bins of length 1 degree Celsius. Moreover, after testing the inclusion of interactions between the two discrete densities and the six regional dummies, we decide to integrate the interactions solely for maximum temperature and two specific regions: RRD, and NCC. As a result, we get $J = 4$ compositional parameters associated with the discrete densities and denoted by $\beta^{max}_{RRD}, \beta^{max}_{NCC}$ and $\beta^{max}_{other}$ for the maximum temperature and $\beta^{min}$ for minimum temperature.

As demonstrated for example in [27], after transformation of the compositional covariates by any transformation in the log-ratio family (isometric or additive log-ratio), the estimation of such a model is done by ordinary least squares. The choice of any of these transformations correspond to a particular parametrization of the same model but yield the same result for the discrete densities contribution when expressed as a linear combination of the logarithm of the histogram bin frequencies (with a zero sum constraint on the coefficients). Although the clr transformation is not adapted to the model fitting step since it would lead to a singular design matrix for the model, it is useful to write the clr version of equation (3) for interpretation purposes:

$$Y_i = \alpha + \sum_{j=1}^{J} < \mathrm{clr}\boldsymbol{\beta}_j, \mathrm{clr}\mathbf{X}_{ij} >_{\mathbb{R}^{L_j}} + \sum_{l=1}^{L} \gamma_l \mathbf{Z}_{il} + \epsilon_i, \tag{4}$$

## 4.2 The smooth regression model

Extending the model in [9] to the case of several density covariates as well as additional scalar covariates, we consider the following linear scalar on density regression model

$$Y_i = \beta_0 + \sum_{j=1}^{J} < \beta_j(t), f_{ij}(t) >_{\mathcal{B}^2([a_j,b_j])} + \sum_{l=1}^{L} \gamma_l \mathbf{Z}_{il} + \epsilon_i, \tag{5}$$

where $Y_i$ is the scalar dependent variable, $\beta_0$ is a real intercept, $\beta_j(t), j = 1, \dots J$ are curve-parameters for the effects of the densities $f_{ij}$, $Z_l$ $(l = 1, \dots, L)$ are real covariates with their corresponding parameters $\gamma_l$, and finally $\epsilon_i$ are normal errors with mean zero and standard deviation $\sigma^2$. The densities $f_{ij}$ as well as the curve-parameters $\beta_j$ are assumed to belong to some Bayes space $\mathcal{B}^2([a_j, b_j])$.

Using the fact that the clr transform is an isometry between $\mathcal{B}^2([a, b])$ and $L^2_0([a, b])$ equipped with their respective inner products, we can rewrite the model as follows

$$Y_i = \beta_0 + \sum_{j=1}^{J} < \mathrm{clr}\beta_j(t), \mathrm{clr}f_{ij}(t) >_{L^2_0([a_j,b_j])} + \sum_{l=1}^{L} \gamma_l \mathbf{Z}_{il} + \epsilon_i. \tag{6}$$

In order to estimate this model, we first need to use a basis expansion of the functional parameters $\beta_j(t)$, as well as a similar expansion for the densities $f_{ij}(t)$. For the sake of simplicity, we will use the same basis system to express the functional regression parameters and the observed functional explanatory variables. The expansion can be written directly in $\mathcal{B}^2([a, b])$ with a basis of CB-splines or equivalently for the clr transforms in $L^2_0([a, b])$ with a basis of ZB-splines. We then replace these functions by their expansions in the inner products of the model equation (5) or (6). Consequently, the inner products terms appear as linear combinations of the beta curves coordinates whose coefficients are given by the product of the Gram matrix (inner products of all pairs of basis functions) by the densities coordinates as in [9]. After this step, we are back to a classical linear model for ordinary covariates that we can fit with ordinary least squares.

As before in our application, all observations are indexed by province $i$ and year $k$ therefore the index $i$ of equation (5) or (6) is replaced by the two indices: $i$ for the province and $k$ for the year. $\beta_0$ is a real intercept and we have the same $L = 7$ classical covariates as for the discrete model (time, precipitation and regional dummies) with their corresponding parameters $\gamma_l$. As for the discrete model, we include two smooth density covariates $f_{ik}^{max}$ and $f_{ik}^{min}$, which are respectively the densities of daily maximum and minimum temperature, in province $i$ and year $k$. To facilitate the comparison, we include the same interactions between densities and regional dummies. The corresponding curve-parameters will be denoted by $\beta_{RRD}^{max}(t), \beta_{NCC}^{max}(t)$ and $\beta_{other}^{max}(t)$ for the maximum temperature and $\beta^{min}(t)$ for minimum temperature. Finally $\epsilon_{ik}$ are normal errors with mean zero and standard deviation $\sigma^2$. $f_{ik}^{max}$, $f_{ik}^{min}$ as well as all the curve-parameters are assumed to belong to some Bayes space $\mathcal{B}^2([a, b])$ ($a$ and $b$ will differ for maximum and minimum temperature).

The number of basis functions for the expansion is a function of the number of knots. In order to reduce variability, it is advisable to use a small number of knots compared to the sample size. Respecting the Schoenberg-Whitney conditions of Section 2.4 and after a few tests, we select $g = 9$ knots corresponding to the dimension $9 + 3 = 12$ for the corresponding ZB-basis. A technical but important detail for comparing the two models is that for a bin of size 1 the discrete inner product of two histograms correspond exactly to their smooth inner product.

Let us note an important difference between the discrete and the smooth model. Conventional compositional data analysis does not pay attention to the order of the components (permutation invariance). However in our case, for a temperature histogram, the components correspond to temperature bins and the order of these bins should be considered in order to take into account some continuity of the bin frequencies with respect to the bins positions on the temperature axis. In contrast the smooth approach does take this into account.

## 4.3 Model results

The histograms smoothing step and the fitting of both models are performed with the R packages *compositions* and *robCompositions*, adapting some codes from [28]. The parameters estimates for classical significant variables displayed in Table 1 are comparable between discrete and smooth models. Moreover, we performed some tests in the discrete model showing that the maximum temperature histograms and minimum temperature histograms are statistically very significant (with p-value less than $10^{-16}$).

The smooth model with 9 knots has a better fit than the discrete one as shown in Figure 9 displaying the distributions of the distance between fitted and observed values for both models.

The interpretation of parameters of a compositional covariate in a scalar on composition model is presented for example in [27]. In the discrete case, as in [29], we

**Table 1** Estimated coefficients associated to regional dummies, total precipitation and year

| Variable | Regression type<br>Discrete regression | <br>Smooth regression (9 knots) |
|---|---|---|
| Constant | $2.62^{***}$ | $2.72^{***}$ |
| | (0.31) | (0.26) |
| Region | | |
| SR | $-1.18^{***}$ | $-1.25^{***}$ |
| | (0.15) | (0.13) |
| MDR | $-0.09$ | $-0.14$ |
| | (0.27) | (0.14) |
| NMM | 0.06 | $-0.09$ |
| | (0.27) | (0.22) |
| NCC | $-0.75^{**}$ | $-0.86^{***}$ |
| | (0.35) | (0.30) |
| RRD | $-0.22$ | $-0.05$ |
| | (0.37) | (0.30) |
| (Reference = CHR) | | |
| Total precipitation | $-0.0002$ | 0.01 |
| (Thousand ml per year) | (0.04) | (0.04) |
| Year | $0.10^{***}$ | $0.10^{***}$ |
| | (0.002) | (0.002) |
| Adjusted $R^2$ | 0.79 | 0.78 |
| Residual Std. Error | 0.56 (df = 1780) | 0.57 (df = 1834) |
| F Statistic | $65.08^{***}$ | $123.46^{***}$ |
| | (df = 109; 1780) | (df = 55; 1834) |
| RMSE | 1.10 | 0.56 |

Note: *, **, and *** mean significant at 10%, 5%, and 1%, respectively

interpret the disparity among clr parameters as indicative of the impact of the corresponding pairwise log-ratios. Figure 10, respectively Figure 11, show the estimated clr parameters for maximum temperature in the discrete model, respectively for minimum temperature. The curves of the different functional parameters $\hat{\beta}_r^{max}$ on Figure 12, respectively $\hat{\beta}^{min}$ on Figure 13, are presented in the functional clr space on the right plot and in the functional Bayes space on the left plot.

First of all let us note that in [29], the authors are searching for the highest contrast between two clr. However in order to take into account the order of the bins, we suggest to only compare neighboring bins. For the RRD region, the fact that the highest clr coefficient corresponds to the temperature bin 31-32 and the next bin 32-33 is negative so that the ratio of bin counts 31-32 versus 32-33 has the highest marginal effect on rice yield according to the model. A similar but smaller pattern appears with the ratio of bin counts 27-28 versus 28-29. These two phenomenons correspond to the oscillations of the smooth clr curve on Figure 12. Similarly, in the NCC region, the most influential contrast occurs between the bins 30-31 and 31-32 (in the reverse direction) and a smaller contrast is visible between bins 28-29 and 29-30. These two effects are also visible on the corresponding smooth clr curves. For other regions, the contrast is between the bins 30-31 and 31-32 and similarly on the smooth clr curves. On the left plot of Figure 12, the temperature intervals of high importance for rice yield appear very clearly for the three regions. Recalling that a hypothetical temperature density

**Fig. 9** Distance between observed and fitted values by models and regions

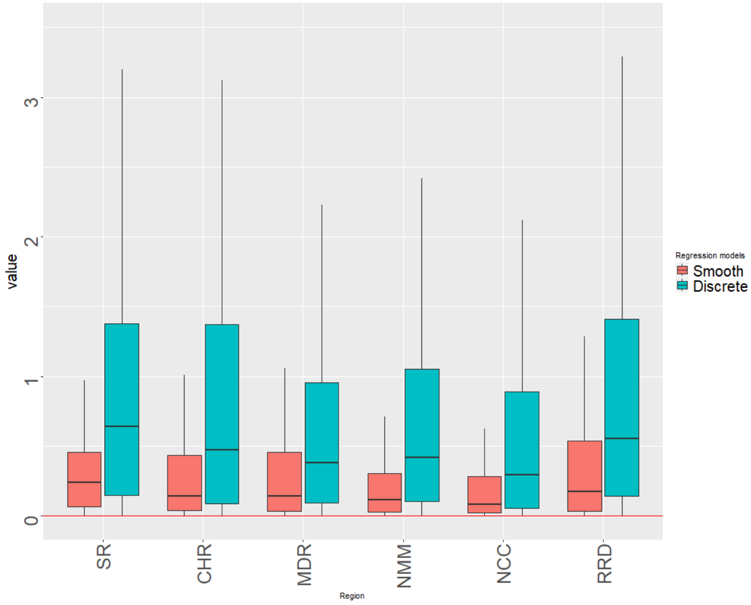

that would correspond to the beta histogram (respectively the beta curve) has highest marginal effect (see [30]), we can conclude that these important intervals correspond to temperatures that are most favorable to rice yield.

Figures 11 (discrete model) and 13 (smooth model) show these parameters for minimum temperature. It is clear that the marginal effects are smaller and that something may be happening in the neighborhood of 25 degrees.

The comparison of the smooth beta curves with their discrete histogram counterparts seem to imply higher maximum values for the smooth curves. This is the same phenomenon as when the smooth density estimate is larger than the histogram counterpart in regions of high density of observations.

The detection of the influential intervals may be affected by the choice of parameters: in the discrete case by the bin size choice and the end-point of the first bin and in the smooth case by the number of knots of the spline approximation. However it is known that a small change in the end-point of the first bin can dramatically affect the histogram whereas the smooth approach is less sensitive to the number of knots. Overall we can say that the results of both models are coherent but more precise and possibly less sensitive to parameter choices for the smooth model.

# 5 Climate change scenario and its marginal effect

We would like to compute projections for the marginal impact of temperature on rice yield corresponding to the IPPC projections of the temperature at the end of this century, see for example [31], and more precisely those projected by RCP2.6.

**Fig. 10** Estimated clr coefficients of maximum temperature for some regions

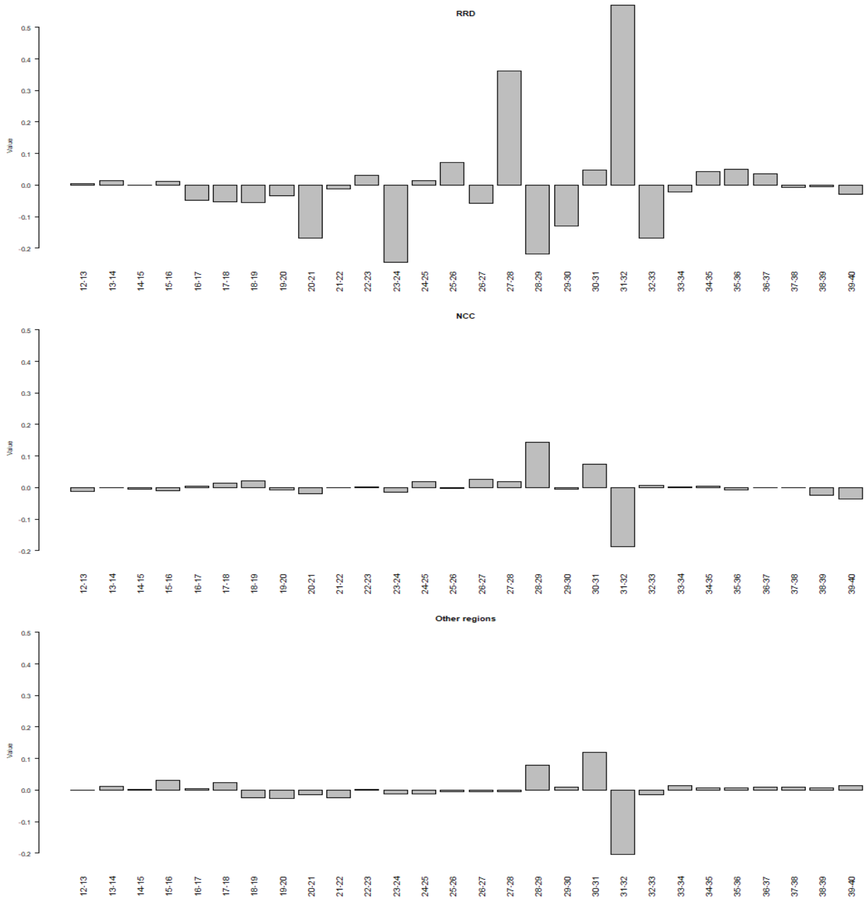

Covariates impact in scalar-on-composition regression can be evaluated either using finite increments as in Coenders and Pawlowsky-Glahn [27] or infinitesimal increments as in Morais et al [32] but the two approaches coincide in this case as can be seen in [33].

In order to assess the impact of a compositional covariate in a model such as (3) or (5), we imagine possible change scenarios for this covariate. To remain coherent with the linear structure of the spaces to which the parameters belong, it is desirable to consider change scenarios that are linear with respect to the vector space structure of the simplex $\mathcal{S}^{28}$ in the discrete case and to the vector space structure of the Bayes space $\mathcal{B}^2([a,b])$ in the smooth case. Let us first look at what are linear changes in these two frameworks.

In the discrete case, the perturbation of a histogram $f$ by a change scenario of direction $\varphi \in \mathcal{S}^{28}$ is given by

$$Tf = f \oplus \varphi, \tag{7}$$

**Fig. 11** Estimated clr coefficients of tmin in the discrete regression

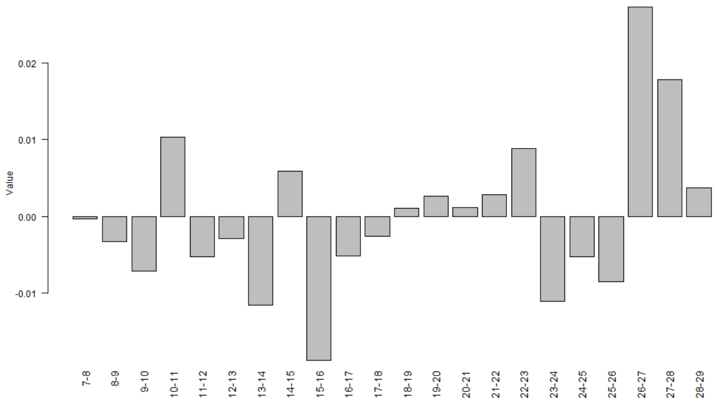

**Fig. 12** Curves of $\hat{\beta}^{max}$ in the smooth regression model with interactions for all regions. Left: in $B^2$, right: in $L^2$

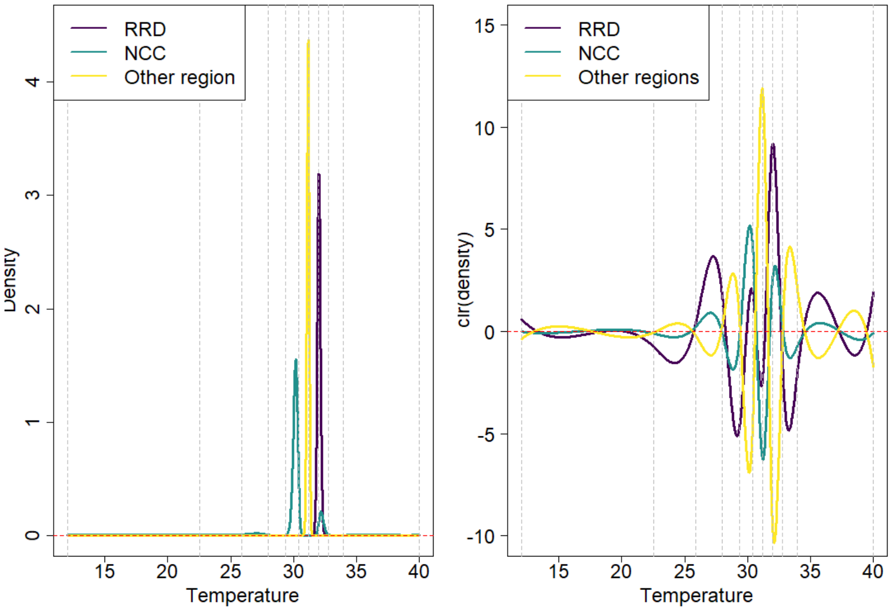

where $\varphi$ is a direction of change in $\mathcal{S}^{28}$. Equivalently we may write $\varphi = Tf \ominus f$, and therefore the change vector is given by $\varphi = \mathcal{C}(\frac{Tf_1}{f_1}, \ldots, \frac{Tf_D}{f_D})$, emphasizing the fact that the components of change vector $\varphi$ from the initial distribution $f$ to $Tf$ describe relative changes in the original scale of frequencies.

**Fig. 13** Curves of $\hat{\beta}^{min}$ in the smooth regression model with interactions for all regions. Left: in $B^2$, right: in $L^2$

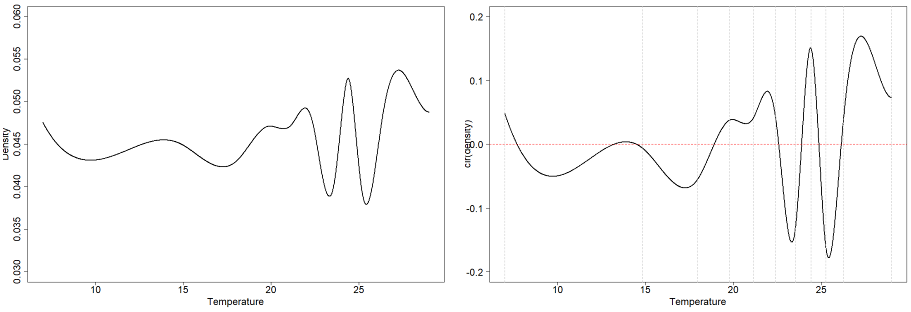

Similarly in the smooth case, and using on purpose the same notation for a different object, the perturbation of a density $f(.)$ by a change scenario $\varphi(.) \in \mathcal{B}^2([a,b])$ is given by

$$Tf(.) = f(.) \oplus \varphi(.). \tag{8}$$

Note that, in clr space, the change is a simple additive change in the discrete case and

$$\text{clr}Tf = \text{clr}f + \text{clr}\varphi \tag{9}$$

and respectively in the smooth case

$$\text{clr}Tf(.) = \text{clr}f(.) + \text{clr}\varphi(.). \tag{10}$$

Since the RCP2.6 projections are available as histograms, we decide to choose a change direction curve in $\mathcal{B}^2([a,b])$ which coincides with a histogram function with bins of length one. Therefore the change curve $\varphi(t)$ is totally determined by the vector of histogram frequencies $\varphi$ used for the discrete model and the climate change scenario is common to both cases.

The changes we consider are the changes between the last observed date 2016 and the end of the century 2099 given by RCP2.6 both for maximum temperature (denoted by $\varphi^{max}$) and minimum temperature (denoted by $\varphi^{min}$). Note that since each province $i$ has its own 2016 histogram and its own RCP2.6 histogram, the resulting change vectors $\varphi_i^{max}$ and $\varphi_i^{min}$ depend on the province. In order to first visualize these changes, we plot some histograms of the RCP2.6 compared to the corresponding 2016 histogram on Figures 14 (for maximum temperature) and Figure 15 (for minimum temperature). The four subplots correspond to the four regions RRD, NCC, CHR and MDR where the regional change has been computed as a simplex average of the province changes in that region.

We observe that for the RRD and NCC regions, it is the temperature bin 32-33 which is experiencing the highest change, whereas it is the bin 31-32 in the MDR region and the bin 29-30 in the CHR region.

**Fig. 14** Maximum temperature distributions in four regions: observed in 2016 and projected by RCP2.6

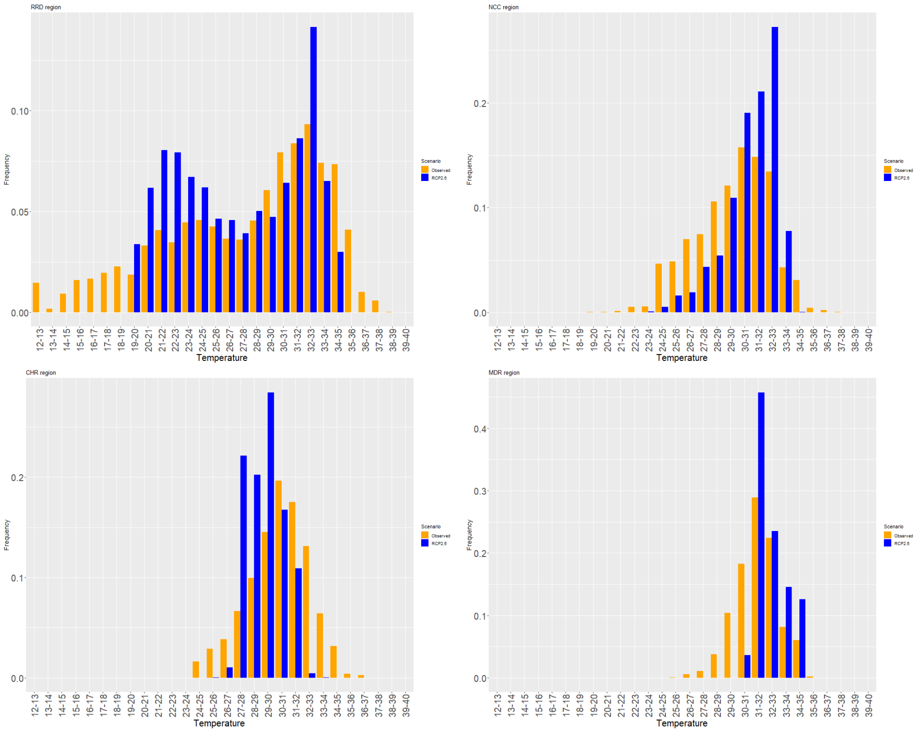

If this hypothetical climate change were to happen in a given province between an initial year, say 0, and year $s$, we are now able to compute a projection of the resulting rice yield change, decomposed into a contribution of the change of the maximum temperature distribution and that of the minimum temperature. Let $\hat{Y}_{is}(\varphi_i^{max}) - \hat{Y}_{i0}$, respectively $\hat{Y}_{is}(\varphi_i^{min}) - \hat{Y}_{i0}$, denote the projected rice yield change due to maximum temperature, respectively minimum temperature, under the change scenario. Given that both our models are linear for the simplex structure and that $Tf_{is}(t) \ominus f_{i0}(t) = \varphi_i(t)$, the resulting change of rice yield due to the change of maximum temperature for a given province $i$ and a given year $s$ are given by

- in the discrete regression model

$$\begin{aligned} \hat{Y}_{is}(\varphi_i^{max}) - \hat{Y}_{i0} &= \sum_{r=1}^{3} \mathbf{1}_{i\in r} < \hat{\beta}_r^{max}, \varphi_i^{max} >_A \qquad (11) \\ &= \sum_{r=1}^{3} \mathbf{1}_{i\in r} < \mathrm{clr}\hat{\beta}_r^{max}, \mathrm{clr}\varphi_i^{max} >_{\mathbb{R}^{28}}, \end{aligned}$$

**Fig. 15** Minimum temperature distributions in four regions: projected by RCP2.6 and observed in 2016

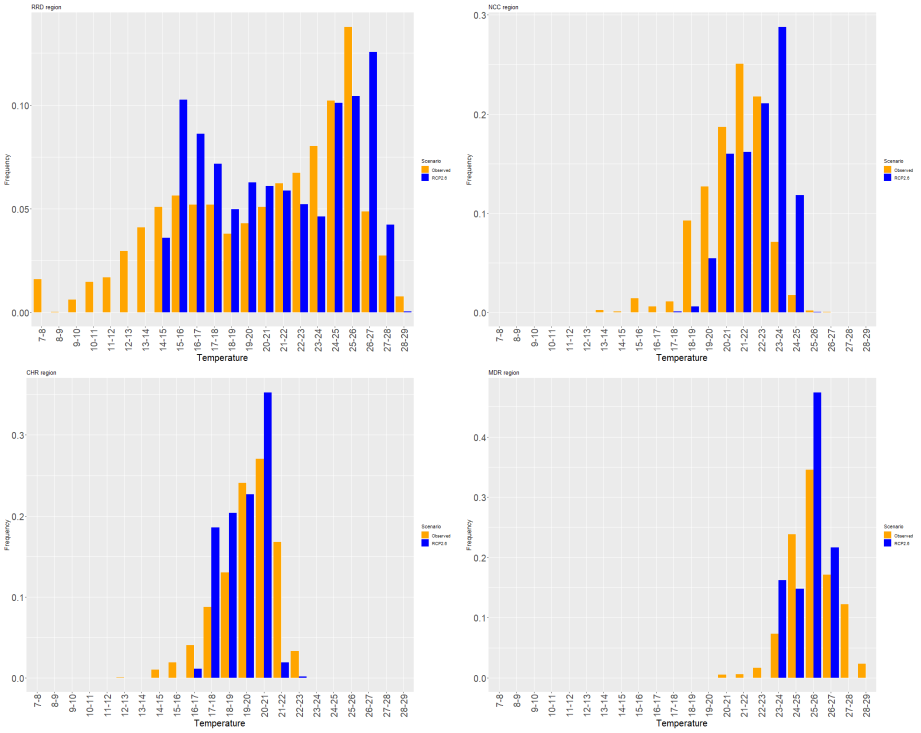

- in the smooth regression model

$$\begin{aligned} \hat{Y}_{is}(\varphi_i^{max}) - \hat{Y}_{i0} &= \sum_{r=1}^{3} \mathbf{1}_{i\in r} < \hat{\beta}_r^{max}(t), \varphi_i^{max}(t) >_{\mathcal{B}^2} \\ &= \sum_{r=1}^{3} \mathbf{1}_{i\in r} < \mathrm{clr}\hat{\beta}_r^{max}(t), \mathrm{clr}\varphi_i^{max}(t) >_{L_0^2}, \end{aligned} \tag{12}$$

Similar formulas can be written for minimum temperature impacts. Note that since a given province belongs to a single region, there is indeed a single non-zero term in the right hand side sums. The inner products $< \mathrm{clr}\hat{\beta}^{max}, \mathrm{clr}\varphi_i^{max} >_{\mathbb{R}^{28}}$, and $< \mathrm{clr}\hat{\beta}^{min}, \mathrm{clr}\varphi_i^{min} >_{\mathbb{R}^{22}}$ in the discrete model, respectively $< \mathrm{clr}\hat{\beta}^{max}(t), \mathrm{clr}\varphi_i^{max}(t) >_{L_0^2}$ and $< \mathrm{clr}\hat{\beta}^{min}(t), \mathrm{clr}\varphi_i^{min}(t) >_{L_0^2}$ in the smooth model therefore characterize the impacts of a change in temperature density in the respective models. The computation of the variance of the impacts is derived in the Appendix. They involve the computation of integrals of the products between the change functions and the ZB spline basis functions. We show that these can be computed easily using the fact that our change functions are step functions combined with the fact that ZB splines of order $d$ are derivatives of B-splines of order $d + 1$, see [10].

Table 2 displays the impacts and their standard error in our application, together with a 95% confidence interval. Concerning the impact of maximum temperature, the smooth model predicts a positive and significant impact in all regions whereas the discrete model only agrees with the smooth model for the NCC region. In other regions, the discrete model effect is either insignificant (for SR, MDR and NMM regions) or disagrees on the sign of the effect.

For minimum temperature, the discrete model concludes with a significant effect only for the CHR and NCC regions whereas the smooth impact is always significant. When they are both significant, they agree on the sign.

**Table 2** Impact of temperature change on rice yield by regions based on RCP2.6

| Type | Region | Discrete regression | | | | Smooth regression | | | |
|---|---|---|---|---|---|---|---|---|---|
| | | mean | lwr | upr | sd | mean | lwr | upr | sd |
| Tmax | SR | 0.22 | -0.45 | 0.65 | 0.63 | 8.53 | 8.51 | 8.54 | 0.02 |
| | CHR | -1.18 | -0.39 | -0.26 | 0.12 | 22.72 | 22.55 | 22.88 | 0.31 |
| | MDR | -0.38 | -0.47 | 0.26 | 0.67 | 8.52 | 8.50 | 8.54 | 0.04 |
| | NMM | 0.07 | -0.08 | 0.12 | 0.19 | 0.42 | 0.34 | 0.50 | 0.14 |
| | NCC | 0.39 | 0.01 | 0.20 | 0.17 | 1.61 | 1.55 | 1.68 | 0.12 |
| | RRD | -2.22 | -1.57 | -0.24 | 0.83 | 10.99 | 10.93 | 11.04 | 0.07 |
| Tmin | SR | 0.10 | -0.00 | 0.09 | 0.05 | 0.52 | 0.51 | 0.53 | 0.01 |
| | CHR | -0.30 | -0.12 | -0.04 | 0.07 | -3.70 | -3.71 | -3.70 | 0.01 |
| | MDR | -0.03 | -0.07 | 0.05 | 0.11 | 0.01 | 0.01 | 0.02 | 0.01 |
| | NMM | 0.05 | -0.02 | 0.04 | 0.06 | 0.42 | 0.40 | 0.44 | 0.04 |
| | NCC | 0.20 | 0.03 | 0.09 | 0.06 | 1.47 | 1.46 | 1.47 | 0.01 |
| | RRD | -0.13 | -0.13 | 0.02 | 0.10 | -1.29 | -1.30 | -1.28 | 0.01 |

We can explain the divergence between the models for the RRD region looking at the sign of the clr of beta coefficients, respectively beta curves, and compare with the shape of the histograms of 2016 and RCP2.6. Indeed Figure 14 shows that for RRD region, the main changes between the histograms of 2016 and that of the end of the century occur approximately for temperatures between 20 and 25 and between 31 and 33. The discrete and the smooth model have the same clr sign in the range 20-25 and 31-32. However the discrete model displays a negative clr sign in the range 32-33 whereas the smooth beta curve has a positive sign in most of this range except in the last 20% of this interval. Since the end of the century projections predict a higher frequency of temperature in the range 32-33 this results in a negative impact for the discrete model but a positive impact for the smooth. We wee that the discrete model is blind to the sign change of the clr occurring in the range 32-33. Overall we observe smaller impacts estimates for the discrete model compared to the smooth. This phenomenon is normal since we can view the discrete model inner products as approximations of the smooth inner products obtained by replacing the integral of the product of clr functions over a given bin by the mean value of the product of clr functions multiplied by the bin length (one here). Therefore, the discrete product of clr values can be seen as approximating the mean values of the corresponding smooth product of clr functions within the bins, resulting in a reduction in size.

# 6 Conclusion

We have proposed and illustrated a procedure for assessing the impact of climate change on rice yield production in Vietnam using scalar on density regression with a discrete and a smooth frameworks. We have derived formulas to evaluate their variances. The smooth or functional approach allows to keep more information from the density objects (notably, the smoothness of their shape is ignored by the discrete model) and is less sensitive to parameter choice. Moreover via the knots position, the smooth approach allows to use a more complete information in the temperature ranges where the data points concentrate.

We consider our illustration as a feasability demonstration which would need refinements in order to derive pragmatic projections. Indeed, a more realistic assessment would require taking into account the cropping season in each region if the cropping season data were available. We did not have these data and moreover dealing with density covariates with varying supports would have resulted in complexity issues from the methodological side. Indeed, varying supports would generate different spline basis for each region.

In order to measure the impact of climate change, we have chosen to consider separately daily maximum and daily minimum temperature. It would be very interesting to use the bivariate density of these two characteristics, thus taking into account their probable correlation. This would require using bivariate constrained splines as in [34].

# 7 Appendix

This appendix provides details about the computation of the impacts and their variance. We derive the impact variance in a general scenario where the change direction curve may depend on province $i$ and will use it for the change scenario given by the simplex-difference between the RCP2.6 histogram and the observed histogram in 2016 for that province. The computation is very similar in spirit for both the discrete and the smooth framework, however the evaluation of the inner products involved is more intricate in the smooth framework. We evaluate separately the impact of maximum temperature and that of minimum temperature, and then add them up to get the impact of climate change. We develop the computation for maximum temperature and the result for minimum temperature is obtained in the same fashion.

In the smooth framework, the impact estimate for maximum temperature between an initial time, say 0, and time $s$, say $s = 2099$, is given, for a province $i$ in region $r$, by

$$\hat{Y}_{is} - \hat{Y}_{i0} = < clr(\varphi_i), clr(\hat{\beta}_r^{max}) >_{L_0^2(a,b)} . \tag{13}$$

Because the RCP scenarios are available as histograms, we will assume that $\varphi_i$ is a step function (constant on each bin with values $(\varphi_i)_j$ for bin $j$.). Since $clr(\hat{\beta}_r^{max})(t) = \sum_{l=1}^{g+3} z_l(\hat{\beta}_r^{max}) Z_l^4(t)$ the impact of maximum temperature for province $i$ in region $r$ is then given by

$$\hat{Y}_{is} - \hat{Y}_{i0} = \sum_{l=1}^{g+3} z_l(\hat{\beta}_r^{max}) \int clr(\varphi_i)(t) Z_l^4(t) dt, \tag{14}$$

where $z(\hat{\beta}_r^{max})$ is the $g+3$ vector of components of the $\hat{\beta}_r^{max}$ curve in the ZB-spline basis and $Z_l^4(t)$ is the $l^{th}$ ZB-spline curve. For $i = 1$ to 63 and $l = 1$ to $g+3$, let us denote by $p_{il}$ the integral term

$$p_{il} = \int clr(\varphi_i)(t) Z_l^4(t)dt \tag{15}$$

and therefore $\hat{Y}_{is} - \hat{Y}_{i0} = \sum_{l=1}^{g+3} z_l(\hat{\beta}_r) p_{il}$.

To compute the $p_{il}$, we take advantage of the fact that $\varphi_i$ are constant on the bins $(b_j, b_{j+1})$ and then of the fact that the integral of a ZB-spline can be obtained with differences of B-splines of a higher order using equation (7) in [10] as follows

$$\begin{aligned} p_{il} &= \int_{12}^{40} clr(\varphi_i)(t) Z_l^4(t)dt = \sum_{j=1}^{28} \int_{b_j}^{b_{j+1}} clr(\varphi_i)_j(t) Z_l^4(t)dt \qquad (16) \\ &= \sum_{j=1}^{28} clr(\varphi_i)_j \int_{b_j}^{b_{j+1}} Z_l^4(t)dt = \sum_{j=1}^{28} clr(\varphi_i)_j \left(B_l^5(b_{j+1}) - B_l^5(b_j)\right) \qquad (17) \end{aligned}$$

Turning now attention to the variance of the estimated impact of maximum temperature, the unbiasedness of the OLS estimates in clr space implies that $\mathbb{E}(z(\hat{\beta}_r^{max})) = z(\beta_r^{max})$. Therefore we have

$$\text{Var}(\hat{Y}_{is} - \hat{Y}_{i0}) = \mathbb{E}\left[\left(\sum_{l=1}^{g+3}(z_l(\hat{\beta}_r^{max}) - z_l(\beta_r^{max}))p_{il}\right)^2\right] \tag{18}$$

Let $P$ be the $63 \times (g+3)$ matrix of elements $p_{il}$. Then the variance of the impact in province $i$ is given by

$$\text{Var}(\hat{Y}_{is} - \hat{Y}_{i0}) = \text{Var} P_{i.} z(\hat{\beta}_r^{max}) = P_{i.} \text{Var}(z(\hat{\beta}_r^{max})) P_{i.}^T, \tag{19}$$

where $P_{i.}$ is the $i^{th}$ row of $P$. We can estimate $\text{Var}(z(\hat{\beta}_r^{max}))$ by the empirical variance-covariance matrix of the parameters estimates.

Because the computation of the variance would be lengthy and difficult to interpret, we decide to approximate it by using a single scenario of change by region thus replacing in (13) the change $\varphi_i$ by the average (in the simplex sense) of the change corresponding to the RCP scenarios of all the provinces in that region. Therefore $p_{il}$ is replaced by $p_{rl}$ when province $i$ is in region $r$ and the matrix $P$ is then $4 \times (g+3)$ resulting in four values for the right hand side of (19).

# Acknowledgement(s)

Part of this work was completed while the authors were visiting the Vietnam Institute for Advanced Study in Mathematics (VIASM) in Hanoï and the authors express their gratitude to VIASM.

## Disclosure statement

No potential conflict of interest was reported by the author(s).

## Funding

Authors acknowledge funding from the French National Research Agency (ANR) under the Investments for the Future (Investissements d'Avenir) program, grant ANR-17-EURE-0010 and the GEMMES project (Agence Française de Développement).

## References

[1] Filzmoser, P., Hron, K., Menafoglio, A.: Logratio approach to distributional modeling. In: Advances in Contemporary Statistics and Econometrics: Festschrift in Honor of Christine Thomas-Agnan, pp. 451–470. Springer, New York City (2021)

[2] Carter, C., Cui, X., Ghanem, D., Mérel, P.: Identifying the economic impacts of climate change on agriculture. Annual Review of Resource Economics **10**(1), 361–380 (2018)

[3] Aitchison, J.: The Statistical Analysis of Compositional Data. Chapman and Hall, London (1986)

[4] Pawlowsky-Glahn, V., Egozcue, J.J., Tolosana-Delgado, R.: Modeling and Analysis of Compositional Data. John Wiley & Sons, Canada (2015)

[5] Hron, K., Filzmoser, P., Thompson, K.: Linear regression with compositional explanatory variables. Journal of Applied Statistics **39**(5), 1115–1128 (2012)

[6] Petersen, A., Zhang, C., Kokoszka, P.: Modeling probability density functions as data objects. Econometrics and Statistics **21**, 159–178 (2022)

[7] Egozcue, J.J., Díaz–Barrero, J.L., Pawlowsky–Glahn, V.: Hilbert space of probability density functions based on aitchison geometry. Acta Mathematica Sinica **22**(4), 1175–1182 (2006)

[8] Boogaart, K.G., Egozcue, J.J., Pawlowsky-Glahn, V.: Bayes Hilbert spaces. Australian & New Zealand Journal of Statistics **56**(2), 171–194 (2014)

[9] Talská, R., Hron, K., Grygar, T.M.: Compositional scalar-on-function regression with application to sediment particle size distributions. Mathematical Geosciences **53**(7), 1667–1695 (2021)

[10] Machalová, J., Talská, R., Hron, K., Gába, A.: Compositional splines for representation of density functions. Computational Statistics **36**(2), 1031–1064 (2021)

[11] Fisher, R.: The influence of rainfall on the yield of wheat in Rothamsted. Philosophical Transactions of the Royal Society of London **213**, 89–142 (1924)

[12] Davis, K.F., Downs, S., Gephart, J.A.: Towards food supply chain resilience to environmental shocks. Nature Food **2**, 54–65 (2021)

[13] Espagne, E., Alexi, D., Ling, T.P.H., Toan, T.L., Thanh, N.-D., Manh-Hung, N., Hà, T.T.N., Truong, T.N., Anh, T.N., Emmanuel, P., Frédéric, T., Quang, C.T., Thanh, Q.V., Toan, C.V., Marie-Noëlle, W.: Climate change in Vietnam: Impacts and adapatation. a COP26 assessment report of the GEMMES Vietnam project. Technical report, Agence Française de Développement, Paris, France, https://www.ird.fr/gemmes-vietnam-report-climate-change-vietnam-impacts-and-adaptation (2021)

[14] Hsiang, S., Kopp, R., Jina, A., Rising, J., Delgado, M., Mohan, S., Rasmussen, D.J., Muir-Wood, R., Wilson, P., Oppenheimer, M., Larsen, K., Houser, T.: Estimating economic damage from climate change in the United States. Science **356**(6345), 1362–1369 (2017)

[15] Schlenker, W., Roberts, M.J.: Nonlinear temperature effects indicate severe damages to U.S. crop yields under climate change. Proceedings of the National Academy of Sciences **106**(37), 15594–15598 (2009)

[16] Ortiz-Bobea, A.: The empirical analysis of climate change impacts and adaptation in agriculture. In: Handbook of Agricultural Economics vol. 5, pp. 3981–4073. Elsevier, The Netherlands (2021)

[17] Battagliola, M.L., Sørensen, H., Tolver, A., Staicu, A.-M.: Quantile regression for longitudinal functional data with application to feed intake of lactating sows. Journal of Agricultural, Biological and Environmental Statistics, 1–20 (2024)

[18] Deryugina, T., Hsiang, S.: The marginal product of climate. Working Paper 24072, National Bureau of Economic Research (2017)

[19] Aragón, F.M., Oteiza, F., Rud, J.P.: Climate change and agriculture: Subsistence farmers' response to extreme heat. American Economic Journal: Economic Policy **13**(1), 1–35 (2021)

[20] Handcock, M.S., Morris, M.: Relative distribution methods. Sociological Methodology **28**(1), 53–97 (1998)

[21] De Boor, C.: A Practical Guide to Splines. Springer, New York (1978)

[22] Schumaker, L.: Spline Functions: Basic Theory. Cambridge University Press, United Kingdom (2007)

[23] Machalova, J., Hron, K., Monti, G.S.: Preprocessing of centred logratio transformed density functions using smoothing splines. Journal of Applied Statistics **43**(8), 1419–1435 (2016)

[24] Machalová, J.: Optimal interpolatory splines using *b*-spline representation. Acta Universitatis Palackianae Olomucensis. Facultas Rerum Naturalium. Mathematica **41**(1), 105–118 (2002)

[25] Burgess, M.G., Ritchie, J., Shapland, J., Pielke, R.: Ipcc baseline scenarios have over-projected co2 emissions and economic growth. Environmental Research Letters **16**(1), 014016 (2020)

[26] Tran-Anh, Q., Ngo-Duc, T., Espagne, E., Trinh-Tuan, L.: A high-resolution projected climate dataset for vietnam: construction and preliminary application in assessing future change. Journal of Water and Climate Change **13**(9), 3379–3399 (2022)

[27] Coenders, G., Pawlowsky-Glahn, V.: On interpretations of tests and effect sizes in regression models with a compositional predictor. SORT–Statistics and Operations Research Transactions **44**(1), 201–220 (2020)

[28] Menafoglio, A.: BayesSpaces-codes. GitHub (2021)

[29] Van den Boogaart, K., Filzmoser, P., Hron, K., Templ, M., Tolosana-Delgado, R.: Classical and robust regression analysis with compositional data. Mathematical Geosciences **53**(5), 823–858 (2021)

[30] Van den Boogaart, K.G., Tolosana-Delgado, R.: Analyzing Compositional Data with R vol. 122. Springer, Berlin (2013)

[31] Scenarios, E.: Ipcc special report. Cambridge Univ, Cambridge (2000)

[32] Morais, J., Thomas-Agnan, C., Simioni, M.: Interpretation of explanatory variables impacts in compositional regression models. Austrian Journal of Statistics **47**(5), 1–25 (2018)

[33] Dargel, L., Thomas-Agnan, C.: Pairwise share ratio interpretations of compositional regression models. Computational Statistics & Data Analysis **195**, 107945 (2024)

[34] Hron, K., Machalová, J., Menafoglio, A.: Bivariate densities in bayes spaces: orthogonal decomposition and spline representation. Statistical Papers **64**(5), 1629–1667 (2023)